

We are IntechOpen, the world's leading publisher of Open Access books Built by scientists, for scientists

6,900

Open access books available

186,000

International authors and editors

200M

Downloads

Our authors are among the

154

Countries delivered to

TOP 1%

most cited scientists

12.2%

Contributors from top 500 universities



WEB OF SCIENCE™

Selection of our books indexed in the Book Citation Index
in Web of Science™ Core Collection (BKCI)

Interested in publishing with us?
Contact book.department@intechopen.com

Numbers displayed above are based on latest data collected.
For more information visit www.intechopen.com



Effects of Quantum-Well Base Geometry on Optoelectronic Characteristics of Transistor Laser

Iman Taghavi and Hassan Kaatuzian
Amirkabir University of Technology (Tehran Polytechnic)
Iran

1. Introduction

Since the discovery of the transistor, the base current (minority carrier recombination) has been the key to the device operation. Among all developments through which Bipolar Junction Transistors (BJT) have progressed, the most innovating modification may be the replacement of the homojunction emitter material by a larger-energy-gap material, thus forming a Heterojunction Bipolar Transistor (HBT). In a silicon bipolar junction transistor, both homo and hetero structures, the base current is dissipated as heat, i.e. through nonradiative recombination, but can yield substantial radiative recombination for a direct-bandgap semiconductor like GaAs. Thus we can reinvent the base region and its mechanism (i.e. carrier recombination and transport function) to decrease current gain significantly and achieve stimulated recombination.

Researches on III-V high-current-density high-speed HBT, revealed the ability of the transistor to operate electrically and optically in the same time. The modified transistor, called in literature as light emitting transistor (LET), works as a three port device with an electrical and an optical outputs (Feng et al. 2004a). Further improvements including wavelength tunability obtained by incorporating a place for better carrier confinement, called a Quantum-Well (QW) (Feng et al. 2004b). Carrier recombination in quantum well (QW) can be modified with a reflecting cavity changing the optoelectronic properties of QWLET (Walter et al. 2004). Room temperature continuous wave operation of such a device at GHz develops a novel three-terminal device, called a HBT Transistor Laser (HBTL) or briefly TL, in which laser emission produces by stimulated recombination (Feng et al. 2005).

In the TL, the usual transistor electrical collector is accompanied with an optical collector, i.e. the above mentioned QW, inserted in the base region of the HBT. Stimulated recombination, unique in the TL, causes "compression" in the collector I-V characteristics and decrease in gain. Combined functionality of an HBT, i.e. amplification of a weak electrical signal, and that of a diode laser, i.e. generating laser emission, is observed in the TL. In other words, a modulating base current leads to modulated signals of the laser output power and collector current. It raises the possibility of replacing some metal wiring between components on a circuit board or wafer chip with optical interconnections, thus providing more flexibility and capability in optoelectronic integrated circuits (OEIC) (Feng et al. 2006a). It has been planned that TL is appropriate for telecommunication and other applications because of its capability of achieving a large optical bandwidth (BW) and a

frequency response without sharp resonance. Processing speed can increase when the TL-equipped microprocessors are commercialized in the future.

Utilizing the I-V characteristics of a TL (Then et al., 2007a) together with common transistor charge analysis, dynamic properties and collector current map are extracted where the above mentioned “compression” is observed in the common emitter gain ($\beta \equiv I_C/I_B$) (Chan et al. 2006). A Transistor Laser with increased (external) mirror reflection demonstrates empirically (Walter et al. 2006) lower threshold current and higher collector breakdown voltage while increased breakdown at lower currents is observed on the collector I-V characteristics if the base region cavity Q is spoiled. Electrical properties of TL will therefore become similar to those of normal transistor ($\beta_{stim} \rightarrow \beta_{spon}$) (Chan et al. 2006). Trade-off between collector current gain and the differential optical gain of a heterojunction bipolar transistor laser TL has been demonstrated analytically before (Then et al. 2009). The electrical-optical gain relationship shows that a reduction in the transistor current gain is accompanied by an increase in the differential optical gain of the TL and, as a consequence, results in a larger optical modulation bandwidth. Another trade-off, i.e. electrical gain-optical bandwidth, has also been reported for which one can utilize in order to extract the maximum possible optical bandwidth of TL (Taghavi & Kaatuzain, 2010).

We proceed in section 2 by introducing the TL crystal structure and fabrication issues, while details are left with proper references for an interested reader. In section 3 carrier dynamics and charge control model in TL will be discussed which is necessary for interpretation of device physics. This section determines a simplified method for analytical modelling of TL and their modifications through the years TL has been invented. TL optical bandwidth and current gain are formulized in the section 4. The method will be utilized in section 5 to simulate QW-base geometry effects on optoelectronic characteristics of the TL. The investigated transistor laser has an electrical bandwidth of more than 100GHz. Thus the structure can be modified, utilizing the methods mentioned in the section 5, to equalize optical and electrical cut-off frequencies as much as possible. Indeed, any improvement in optoelectronic characteristics of TL, i.e. optical bandwidth and current gain, is currently necessary in order to incorporate the TL in OEIC's. The most urgent work needed in the future is an investigation of other quantum-well parameters effect on TL characteristics. Among these parameters are width and number of quantum wells. Section 6 is devoted to discussions about new researches in the field of TL including MQWTL. The chapter will be completed with conclusion in this section.

2. TL structure

The device studied here is based on n-p-n heterojunction bipolar transistor (n-InGaP/ p-GaAs +InGaAs quantum well/n-GaAs). The epitaxial structure of the crystal used for the HBTL, demonstrated in Fig. 1, consist of a 5000 Å n-type heavily doped GaAs buffer layer, followed by three layers of n-type forming the bottom cladding layers. These layers are followed by an n-type subcollector layer, a 600 Å undoped GaAs collector layer, and an 880 Å p-type GaAs base layer (the active layer), which includes (in the base region) a 120 Å InGaAs QW (designed for $\lambda \approx 1000$ nm). The base area is $\approx 4000 \mu\text{m}^2$ and we can treat the QW base region as three distinct subregions: Two 10^{19} cm^{-3} doped GaAs regions and one 160 Å undoped InGaAs QW within them. The epitaxial HBTL structure is completed with the growth of the n-type emitter and upper cladding layers. Finally, the HBTL structure is capped with a 1000 Å heavily doped n-type GaAs contact layer. The HBTL fabrication

process utilizes eight mask layers for three wet chemical etching steps, three dry (plasma) etching steps, and three metallization steps for top-side contacts. The HBTL sample is cleaved front-to-back using conventional etching methods to a length of $150\mu\text{m}$ between Fabry-Perot facets. Detailed fabrication process of HBTL has been described in (Chan et al., 2006; Feng et al., 2005; Feng et al., 2006a).

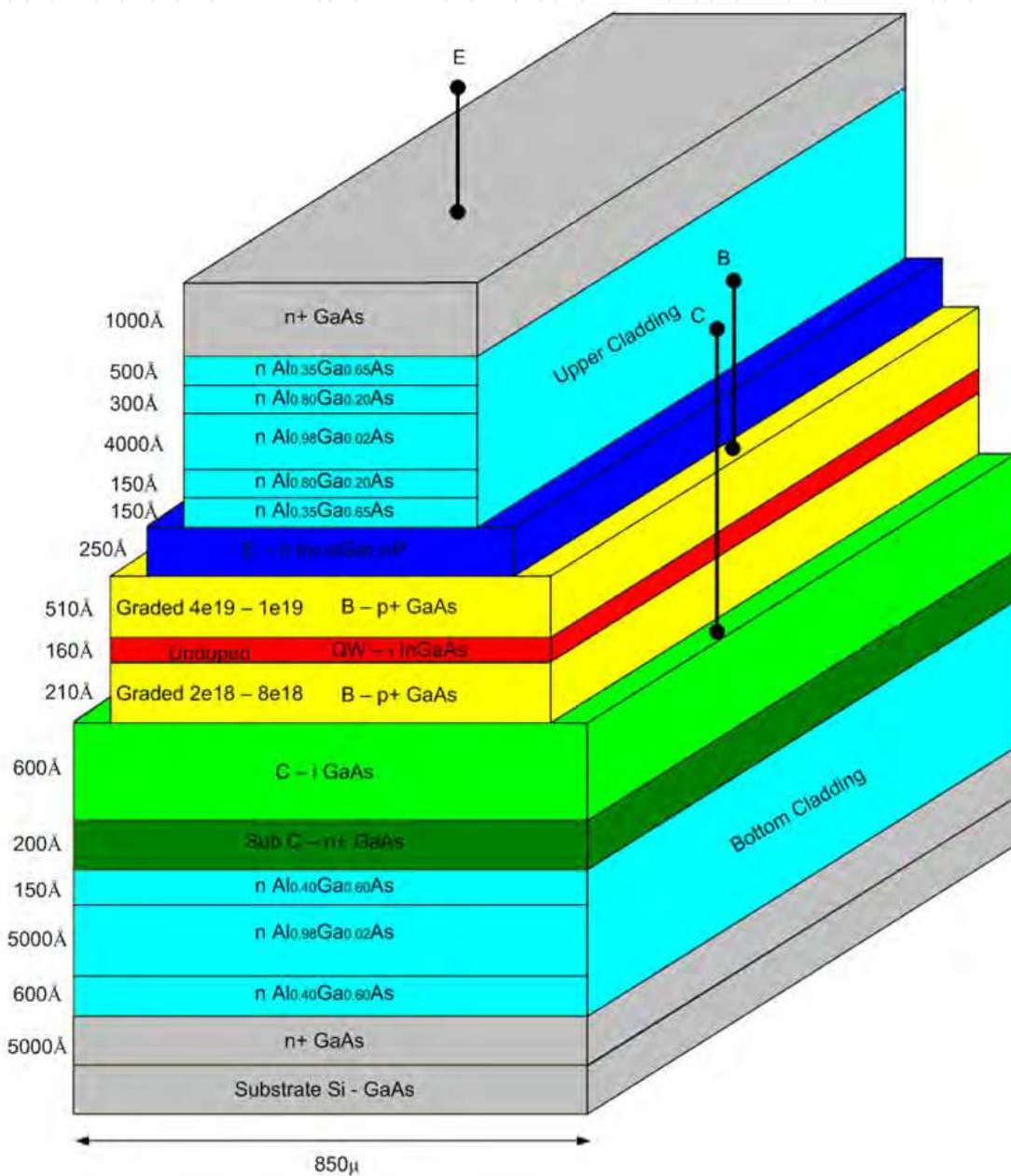


Fig. 1. Epitaxial structure of heterojunction bipolar Transistor Laser (HBTL). A QW is incorporated within the base to improve the recombination efficiency.

Although other device structures like Tunnel Junction Transistor Laser (TJTL)(Feng et al., 2009), VSCEL (Shi et al., 2008), Heterojunction Field effect (HFETL)(Suzuki et al., 1990) and Distributed Feedback Transistor Laser (DFBTL)(Dixon, 2010) have been proposed in the literature, we focus solely on Heterostructure Bipolar Junction transistors.

3. Charge analysis

The three-terminal TL is fundamentally different from a diode laser (single p-n junction), i.e. a two-terminal device, where the injection current is carried totally by recombination. There is no third terminal and collector current “competition”. In TL the collector current I_C ($I_E=I_B+I_C$) is the fraction of emitter current “collected” at the reverse-biased base collector junction, with the remainder I_B supplying base recombination radiation. We show here that the carrier lifetime can be extracted from the HBT I-V characteristics, thus allowing the intrinsic optical frequency response of the TL to be derived by modifying the coupled carrier-photon rate equations.

3.1 Carrier dynamics

Being an essential feature of transistor operation, QW-base recombination of electron-hole supported by the base current I_B causes photon generation while carrier injection into the base region is provided by the emitter current I_E . Solving the continuity equation for the above mentioned three regions of QW-base, expressed in equations 1 and 2 for base bulk and QW region respectively, can shape distribution of base injected electrons from emitter.

$$\partial n/\partial t = D \partial^2 n/\partial x^2 - n/\tau_{bulk} \quad (\text{bulk base}) \quad (1)$$

$$\partial n/\partial t = D \partial^2 n/\partial x^2 - n/\tau_{qw} \quad (\text{QW}) \quad (2)$$

Where $n=n(x,t)$ is the base electron distribution and the quantities τ_{bulk} and τ_{qw} are the recombination lifetimes in the GaAs and in the InGaAs QW, respectively. Sudden decrease in τ_{qw} at lasing threshold is a result of faster recombination rate in the QW thus base carrier tilt at emitter is intensified compared to spontaneous emission. The term n/τ_{qw} in equation 2 represents for spontaneous and stimulated photon generation and coupling of the optical field into the device operation. The bulk lifetime, τ_{bulk} in the GaAs layer with 10^{19} doping is approximated as 193 ps. Uniform diffusion constant, $D \approx 26 \text{ cm}^2/\text{s}$, is assumed throughout the base region and diffusion current, $I=qAD\partial n/\partial x$, is supposed continuous across the GaAs/InGaAs-QW/GaAs interface. The position of QW, W_{EQW} , is assessed here by its central location distance from the emitter-base interface and is the variable parameter during analysis of section 5 where the effect of QW position will be investigated.

Zero charge density at collector-base junction and $\partial n/\partial t=0$ form the initial conditions for the continuity equations 1 and 2. The calculated charge distribution for increasing base current (I_B) corresponding to the I-V characteristics of HBTL are shown plotted in Fig.2. The device currents are then calculated from common formula for diffusion current. Deviation from triangular approximation is observed in Fig. 2 and the profile is inclined more steeply upward near the emitter-base interface due to faster recombination in QW compared with the bulk base and reduced base width ($W_{QW}<W_{EC}$). At the lasing threshold, τ_{qw} decreases abruptly agreeing with $\beta_{stim}<\beta_{spon}$ as stimulated recombination speeds up the overall rate of recombination in the QW. Consequently, the emitter-end “tilt” of the carrier population is more noticeable beyond the threshold.

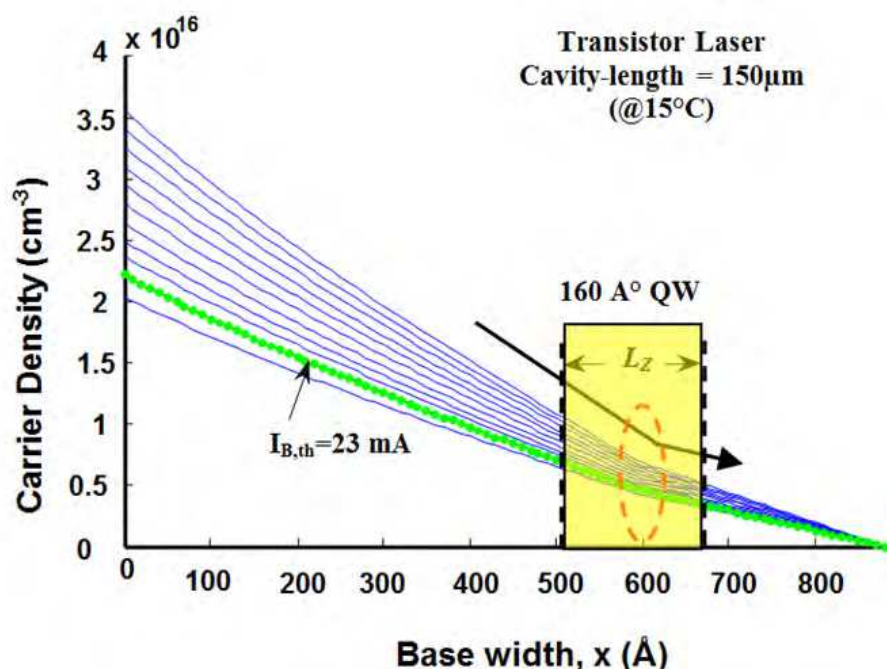


Fig. 2. Calculated minority carrier distribution for increasing I_B corresponding to the I-V characteristics. The shape tilts inside the QW due to faster recombination and reduced base width.

3.2 Charge control model

Charge control model for TL consists of superposition of two different triangular charge populations named as Q_1 and Q_2 (Feng et al., 2007). As TL integrates two distinguish operations, i.e. HBT electrical and semiconductor diode laser optical outputs, it might be supposed as a two-collector device. One is the base-collector junction and the other is QW called correspondingly electrical and optical collector. In the model of charge control Q_1 and Q_2 are responsible for transporting minority carriers to the QW (for optical operation) and keeping transport of carriers to the electrical collector (for electrical operation) respectively. Q_1 and Q_2 are obtained from carrier density profile, Fig. 3 and calculated so that

$$Q_1 = q\Delta n_1 A W_{EQW} / 2 \quad (3)$$

$$Q_2 = q\Delta n_2 A W_B / 2 \quad (4)$$

Where Δn_1 and Δn_2 are extracted from bias data, i.e. emitter base bias voltage (V_{BE}) and I_C , so that $(\Delta n_1 + \Delta n_2)$ exhibits total carrier density at the emitter-base interface. Deriving I_C and I_B from I-V characteristics of TL ($W_{EQW} = 590 \text{ \AA}$), we can estimate Q_1 and Q_2 as

$$I_C = Q_2 / \tau_{t,2} \quad (5)$$

$$I_B = (Q_1 + Q_2) / \tau_{bulk} + Q_1 / \tau_{t,1} \quad (6)$$

Where $\tau_{t,1}$ is the transient time from emitter to QW and $\tau_{t,2}$ is the transient time across the entire base ($W_B = 880 \text{ \AA}$) and calculated as below.

$$\tau_{t,1} = W_{EQW}^2 / 2D \approx 0.67 \text{ ps} \quad (7)$$

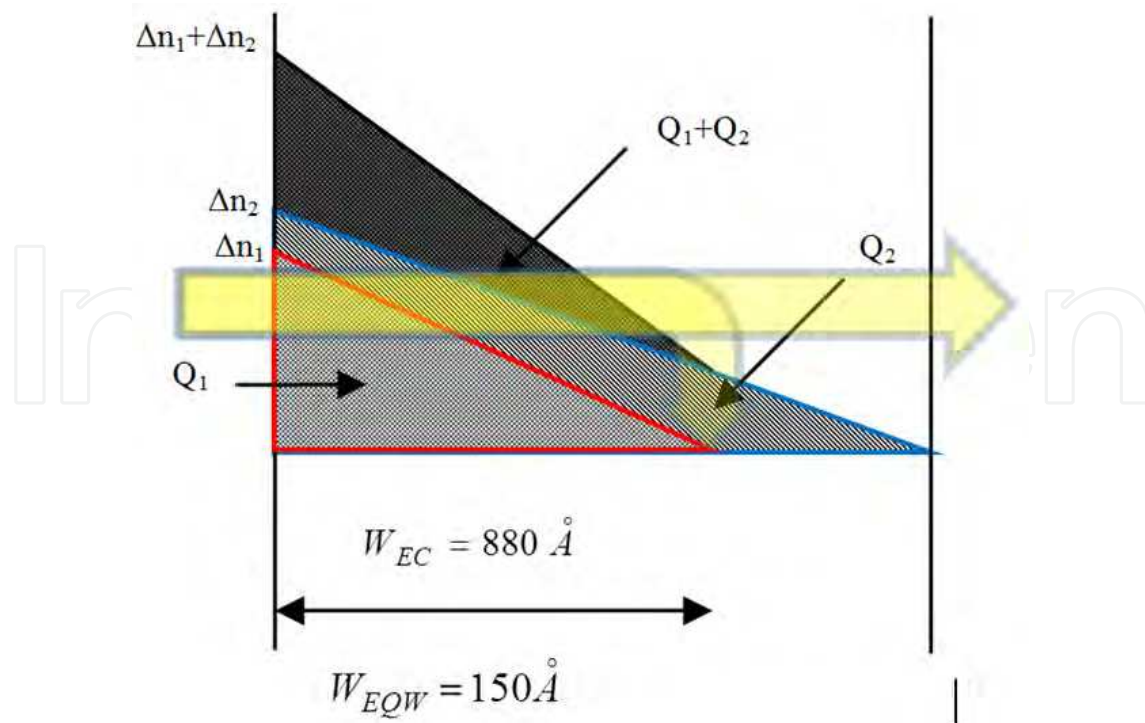


Fig. 3. Charge Control Model illustrates the role of Q_1 and Q_2 triangles in the entire base carrier distribution. Large amount of carriers enter the base while a little of them survive to the collector.

$$\tau_{t,2} = W_B^2/2D \approx 1.5ps \quad (8)$$

Two base carrier populations, Q_1 and Q_2 , are combined to form the overall effective base recombination lifetime, τ_B , of the entire base population which is expressed as

$$1/\tau_B = 1/\tau_{bulk} + \tau_{t,2} Q_1/(Q_1 + Q_2) \quad (9)$$

Since $\tau_{bulk} \gg \tau_{t,1}$, $\tau_B \approx (1+Q_2/Q_1) \cdot \tau_{t,1}$. Beyond the lasing threshold, τ_B decreases when stimulated emission accelerates the overall rate of recombination in the base of the TL. This is obvious in the steeper slope of the Q_1 population, transporting a larger proportion of the base carriers to a faster ($\tau_{B,stim}$) optical collector (QW), leading to a shorter overall base recombination lifetime, τ_B , and decreased gain β . τ_B values for charge density distributions near the threshold and beyond, plotted in Fig. 4 of (Feng et al., 2007).

4. Device optoelectronic characteristics

Among several characteristics, either optical or electrical, of the TL, small signal optical frequency response and current gain are most interesting. The reason arises from the fact that the TL needs suitable optoelectronic characteristics to be incorporated in an Optoelectronic Integrated Circuit (OEIC). The intrinsic frequency response of the TL can be improved towards 100 GHz owing to carrier lifetime determined by a thin base and the ability of the TL to inject and withdraw stored charge within picoseconds (forcing recombination to compete with E-C transport). Methods are required to improve the optical bandwidth to equalize both bandwidths as much as possible. The following describes a brief analysis of these characteristics.

4.1 Small-signal analysis of optical frequency response

When integrated over the entire base width, continuity equations (1) and (2) can result in an approximation for optical frequency response. The result for the TL is a modification of the coupled carrier-photon equations, formulated by Stutz & deMars (Feng et al., 2007) which is expressed as

$$dN/dt = I_E/q - (I_C/q) + N/\tau_{B,spont} + vg\Gamma N_p \quad (10)$$

$$dN_p/dt = vg\Gamma N_p - N_p/\tau_p \quad (11)$$

Where $N \approx (Q_1 + Q_2)/q$ is the total base minority carrier population, v is the photon group velocity, Γ is the optical confinement factor of active medium (i.e. QW), τ_p is the photon lifetime, g is the gain per unit length of the active medium, and N_p is the total generated photon number. The small signal optical frequency response is obtained as below

$$\frac{\Delta P_m(\omega)}{\Delta I_B(\omega)} = \frac{\Gamma_b \tau_p / (qAW_B)}{[1 - (\omega/\omega_n)^2] + j2(\omega/\omega_n)\xi} \quad (12)$$

Where $\Delta P_m(\omega)$ is the modulated photon density, $\Delta I_B(\omega)$ is the modulated base current and Γ_b is the optical confinement factor of the waveguide. The natural frequency and damping ratio are:

$$\omega_n^2 \approx (1/\tau_p \tau_{B,spont})(I_B/I_{B,th} - 1) \quad (13)$$

$$\xi = (2\omega_n \tau_{B,spont})^{-1} + 0.5(\omega_n \tau_p) \quad (14)$$

For $\zeta \leq 0.7$ the resonance frequency and bandwidth are:

$$\omega_r = \omega_n \sqrt{1 - 2\xi^2} \quad (15)$$

$$\omega_{-3db} = \omega_n \sqrt{(1 - 2\xi^2) + \sqrt{4\xi^4 - 4\xi^2 + 4}} \quad (16)$$

While these values for $\zeta \geq 0.7$ are expressed as:

$$\omega_r = 0 \quad (17)$$

$$\omega_{-3db} = \omega_n \sqrt{(1 - 2\xi^2) + \sqrt{4\xi^4 - 4\xi^2 + 2}} \quad (18)$$

We can obtain τ_p from the common equation:

$$1/\tau_p = \left(\frac{c}{n}\right) \{\alpha_i + (1/2L)\ln(1/R_1 R_2)\} \quad (19)$$

For cleaved cavity laser of lengths $L=150$ and $400(\mu\text{m})$ with $R_1=R_2=0.32$ and a photon absorption factor (α) of 5cm^{-1} , the approximate photon lifetime are $\tau_p=1.5$ and $3.6(\text{ps})$ respectively. It should be noticed that we neglect the capture and escape lifetimes in this small signal analysis. Optical gain is also assumed independent on photon and carrier populations. Although the difference in final results is negligible, an interested reader can refer to (Faraji et al., 2009) for more information.

In equations (13) and (14) the parameter $\tau_{B,spont}$ is a specific value of overall base recombination lifetime, τ_B , evaluated in spontaneous emission region at lasing threshold. According to Fig. 4

of (Feng et al.,2007) (not shown here) this value for a TL with $W_{EQW}=590\text{\AA}$ is about 2.5ps. Under bias condition such that $I_B=33\text{mA}$ ($I_B/I_{B,th}=1.5$), small signal optical frequency response for two TL with above mentioned cavity length is sketched in Fig. 4. For comparison, the curve also contains optical response of an ordinary diode laser (DL) with a large base recombination lifetime of $\tau_{B,spn}=100\text{ps}$. When compared with traditional diode laser, fast modulation response of TL is due to this difference in their optical frequency response which suffers a resonance peak in low frequencies in the case of diode laser.

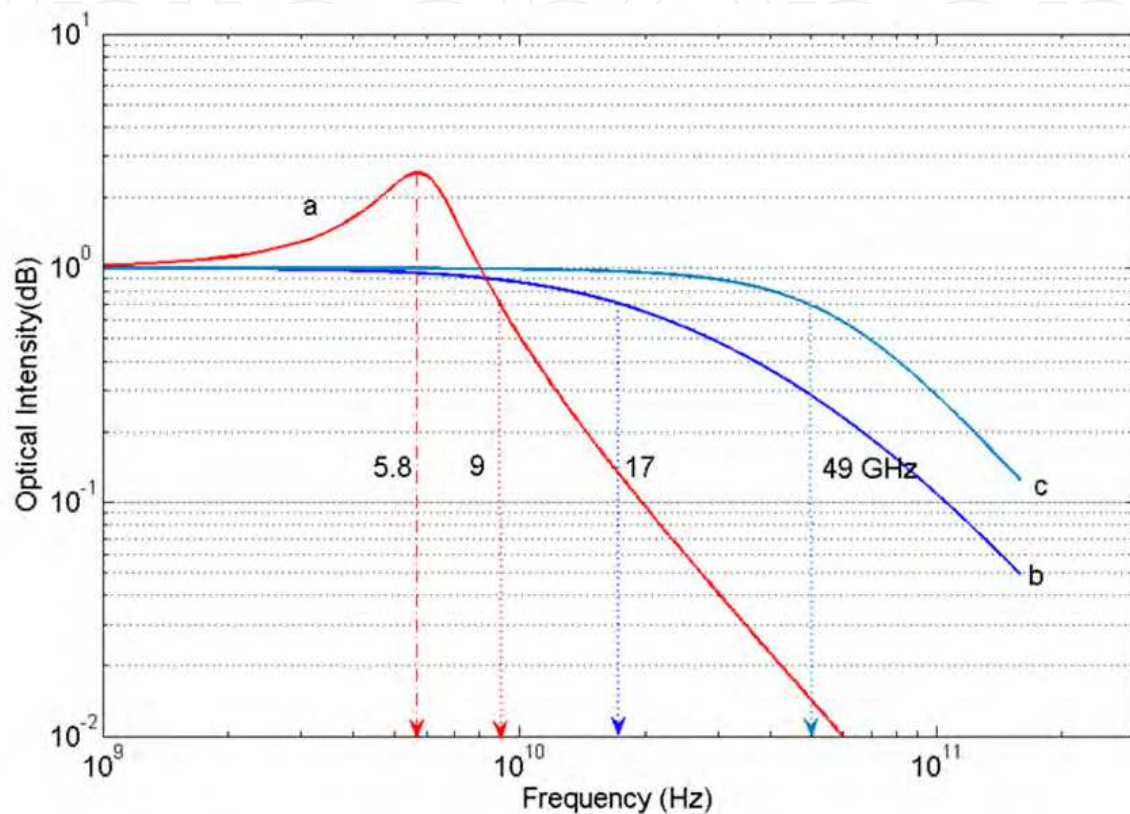


Fig. 4. Small signal optical frequency response of (a) Diode laser with $L=400\mu\text{m}$ ($\tau_{B,spn}=100\text{ps}$), (b) TL with $L=400\mu\text{m}$ ($\tau_{B,spn}=2.5\text{ps}$), (c) TL with $L=150\mu\text{m}$ ($\tau_{B,spn}=2.5\text{ps}$)

The very short effective carrier lifetime of a TL, i.e. the same order of magnitude as the cavity photon lifetime, results in a near unity resonance peak and provides in effect a significantly larger bandwidth, which is typically not available when the bandwidth is limited by carrier-photon density resonance, as in a diode with a large carrier lifetime (0.1–1ns). We see that by charge analysis, if a QW base HBT is capable of laser operation, its “speed” of operation is not affected by common recombination, and the limitation of spatial charge “pileup” as in a diode, but by the base dynamics of charge transport described in this section. Indeed, only fast recombination is able to compete with fast collection of carriers.

4.2 Current gain

Thanks to special features of QW incorporated in its base region, the most recent form of laser, the Transistor Laser, govern carrier recombination and hence electrical current gain, $\beta=\Delta I_C/\Delta I_B$. This gain therefore becomes a crucial parameter in both transistor and laser operations of TL. As previously mentioned, stimulated emission, an extra feature of transistor, makes the collector I-V characteristics “compressed” and decreases β . The gain

value for both the transistor laser and an ordinary HBT (i.e. a Q-spoiled TL) was demonstrated in Fig. 6 of (Walter et al., 2006). Charge control analysis can be utilized in conjunction with these values of current gain to determine the TL terminal currents and estimate base transit and recombination lifetimes. Conversely, one can calculate theoretically β for a TL as described below.

The base and collector currents and the static common-emitter current gain are given for an HBT as

$$I_E = I_B + I_C = Q_B/\tau_B + Q_B/\tau_t \quad (20)$$

$$\beta \equiv \Delta I_C/\Delta I_B = I_C/I_B = \tau_B/\tau_t \quad (21)$$

where Q_B is the charge stored in the base, τ_B is the base recombination lifetime, and τ_t is the base transit time. For the same HBT with a quantum well inserted in the base, a QWHBT, the base current and current gain can be modified and expressed as

$$I_B \equiv I_{BQW} = (Q_B/\tau_B + Q_B/\tau_{QW}) = (Q_B/\tau_{BQW}) \quad (22)$$

$$\beta_{QW} = \tau_{BQW}/\tau_t \quad (23)$$

where τ_{QW} is the recombination lifetime of the quantum well while τ_{BQW} is the effective recombination lifetime of the base and quantum well. For an QWHBT transistor laser with stimulated base recombination, a QWHBTL, the base current and current gain can be further modified and expressed as

$$I_B \equiv I_{BTL} = (Q_B/\tau_B + Q_B/\tau_{QW} + Q_B/\tau_{st}) = (Q_B/\tau_{TL}) \quad (24)$$

$$\beta_{TL} = \tau_{TL}/\tau_t \quad (25)$$

where τ_{TL} is the effective base recombination lifetime of the transistor laser including τ_{st} , the stimulated recombination lifetime.

5. QW-base geometry effects

Since the first report of successful operation of TL, a number of publications reported different material combinations (Dixon et al., 2006), incorporation of Quantum Well(s) (QW) in the base, modulation characteristics (Then et al., 2009)(Feng et al., 2006)(Then et al., 2007b), use of tunnel junctions (Feng et al., 2009), electrical-optical signal mixing and multiplication (Feng et al., 2006a), etc. Various schemes have also been employed to increase the modulation bandwidth of the TL (Then et al., 2008)(Taghavi & Kaatuzian, 2010). A proposal has also been put forward to use the gain medium as an optical amplifier. Several models have appeared in the literature for terminal currents, gain, modulation bandwidth, etc. of TL (Feng et al., 2007)(Faraji et al., 2008)(Basu et al., 2009)(Then et al., 2010)(Zhang & Leburton, 2009). However, these models based on rate equations, give values for optoelectronic characteristics of TL. In addition, the TL has been simulated both numerically (Shi et al., 2008)(Kaatuzian & Taghavi, 2009) and by CAD, i.e. software packages, (Shi et al., 2008)(Duan et al., 2010).

The electron recombination plays an important role in determining the base current due to spontaneous and stimulated emission in the QW, so that the electronic characteristics of the

TL have a strong dependence on its laser operation. This is proved by the decrease in the electrical gain $\beta = \Delta I_C / \Delta I_B$ due to enhanced carrier recombination in the base region when stimulated emission occurs. According to the model described in section 4, effects of geometrical parameters of QW-base on small signal optical frequency response and current gain should be significant. In other words optoelectronic characteristics of TL are directly affected by parameters like QW position in the base (W_{EQW}), well width (W_{QW}) (and barrier width in the case of multiple quantum-wells TL), number of QWs, base width (W_B), etc. For instance, TL characteristics depend on the relative position of QW because of the quasi-linear density profile of the base minority carriers (Fig. 2). Although, the mentioned first order model of charge control does not distinguish between bulk and QW carriers, TL characteristics dependency on QW and base width are still acceptable. Herein, we utilize analysis described in section before to model the effect of QW position on optical bandwidth and current gain of TL. As a goal, we look for an enhanced performance for the TL by “restructuring” it.

5.1 QW location effect

Being integrated inside the base region of the TL, the quantum-well structural parameters have certainly significant influence on both optical and electrical properties of TL, e.g. gain and bandwidth for optical and electrical outputs. This subsection is dedicated to the mentioned effects while other parameters will be studied later.

5.1.1 Carrier profile

According to the model, constant base-emitter voltage and collector current makes ($\Delta n_1 + \Delta n_2$), Δn_1 , Q_2 unchanged. Altering the position of QW within the base can therefore change Q_1 , i.e. portion of carriers responsible for lasing. The new values for Q_1 and $\tau_{t,1}$ (base transit time) when QW moves are as below

$$Q_{1,new} = Q_1 * (W_{EQW,new} / W_{EQW,old}) \quad (26)$$

$$\tau_{t,1,new} = \tau_{t,1,old} * (W_{EQW,new} / W_{EQW,old})^2 \quad (27)$$

For the TL described in previous sections we may set $W_{EQW,old} = 590 \text{ \AA}$. As a result, minority carrier profile of base region solved analytically for $W_{EQW} = 150 \text{ \AA}$ is sketched in Fig. 5. Also Fig. 6 demonstrates the modified charge control model. Displacement of QW position, W_{EQW} , towards emitter can cause two noteworthy effects simultaneously. First, τ_B falls due to reduction of Q_1 while Q_2 is constant. Second, in accordance to the diffusion formula for I_E and Fig. 6, I_E would increase significantly as a result of steeper charge density profile at the base emitter interface.

These conditions make base current (I_B) to rise abruptly beyond the threshold current (22 mA). Due to (Kaatuzian, 2005) the threshold current is constant during this movement of QW. In other words, moving the QW in this direction decreases the electrons which are “trapped” and recombined with holes within it. Thus more carriers are allocated to electrical operation and fewer involved in light generation, i.e. fewer photons created within the well. This phenomenon, exhibited by animation in Fig. 7, means that carriers arrive sooner at QW. As a result of “faster rich time” of minority carriers to the well, it is predicted that both τ_B and β decreases drastically (by about 4 or 5 times for τ_B).

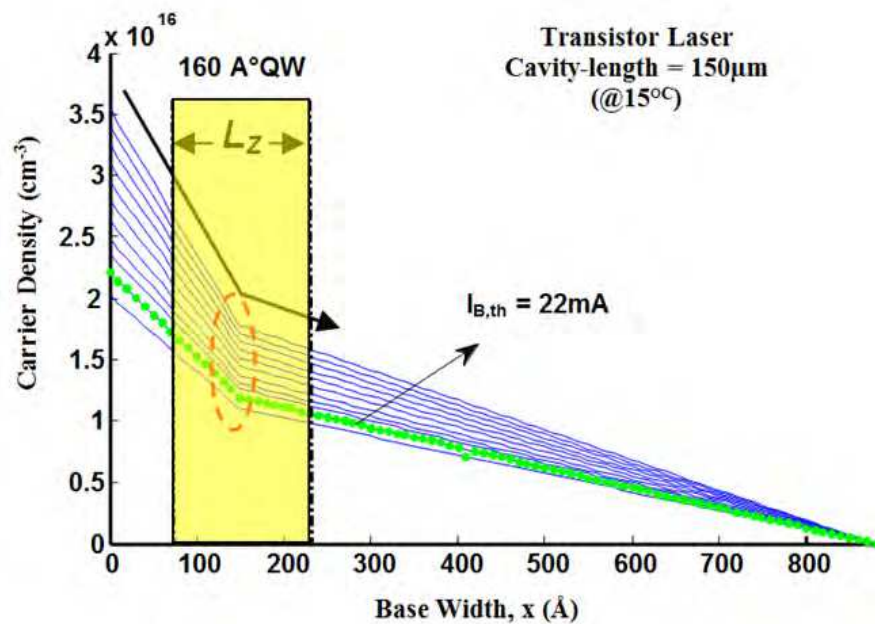


Fig. 5. Calculated minority carrier distribution for QW moved toward emitter; the profile deviates more from triangular form of regular HBT.

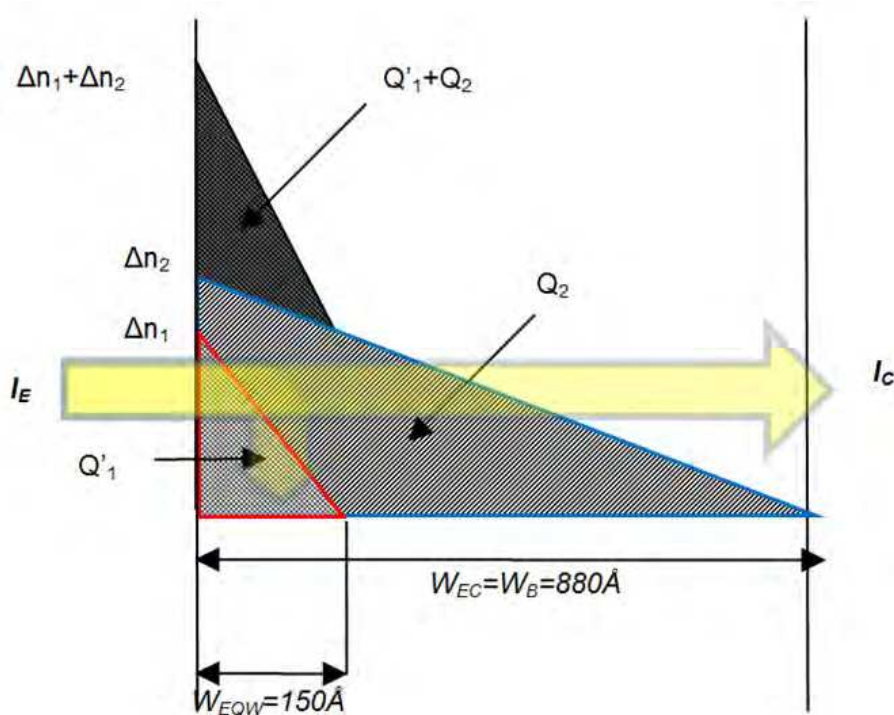


Fig. 6. Modified charge control model for $W_{EQW}=150\text{\AA}$. Q_2 is constant while Q_1 decreased to Q'_1 .

5.1.2 Base recombination lifetime

Overall effective base recombination lifetime of the entire base population, τ_B , can be calculated using the concept of charge control model and is changed for different QW

locations, i.e. W_{EQW} . The special calculation method of τ_B value for different base currents is based on a reverse estimation of them from experimental data for $W_{EQW}=590\text{\AA}$ and the charge relations (physical model). The method involves a set of calculations which generates new values of τ_B using old values of τ_B (i.e. Fig. 4 in (Feng et al., 2007)) and charge relations according to the charge control model of section 3. The result for new τ_B values at $I_B=22\text{mA}$, i.e. $\tau_{B,spont}$ which equals τ_B evaluated at I_{Bth} for QW located in different places through the bulk base is sketched in Fig. 8. To show the reliance of base recombination lifetime on I_B and W_{EQW} simultaneously, τ_B has been drawn in three dimensions (3D) in Fig. 9. Assessing these two figures, it is obvious that the closer to the collector the QW, the less variant with I_B the τ_B . Spontaneous base recombination lifetime ($\tau_{B,spont}$) is obtained by cross section of 3-D scheme of τ_B and $I_B=I_{th}=22\text{mA}$ plane as well.

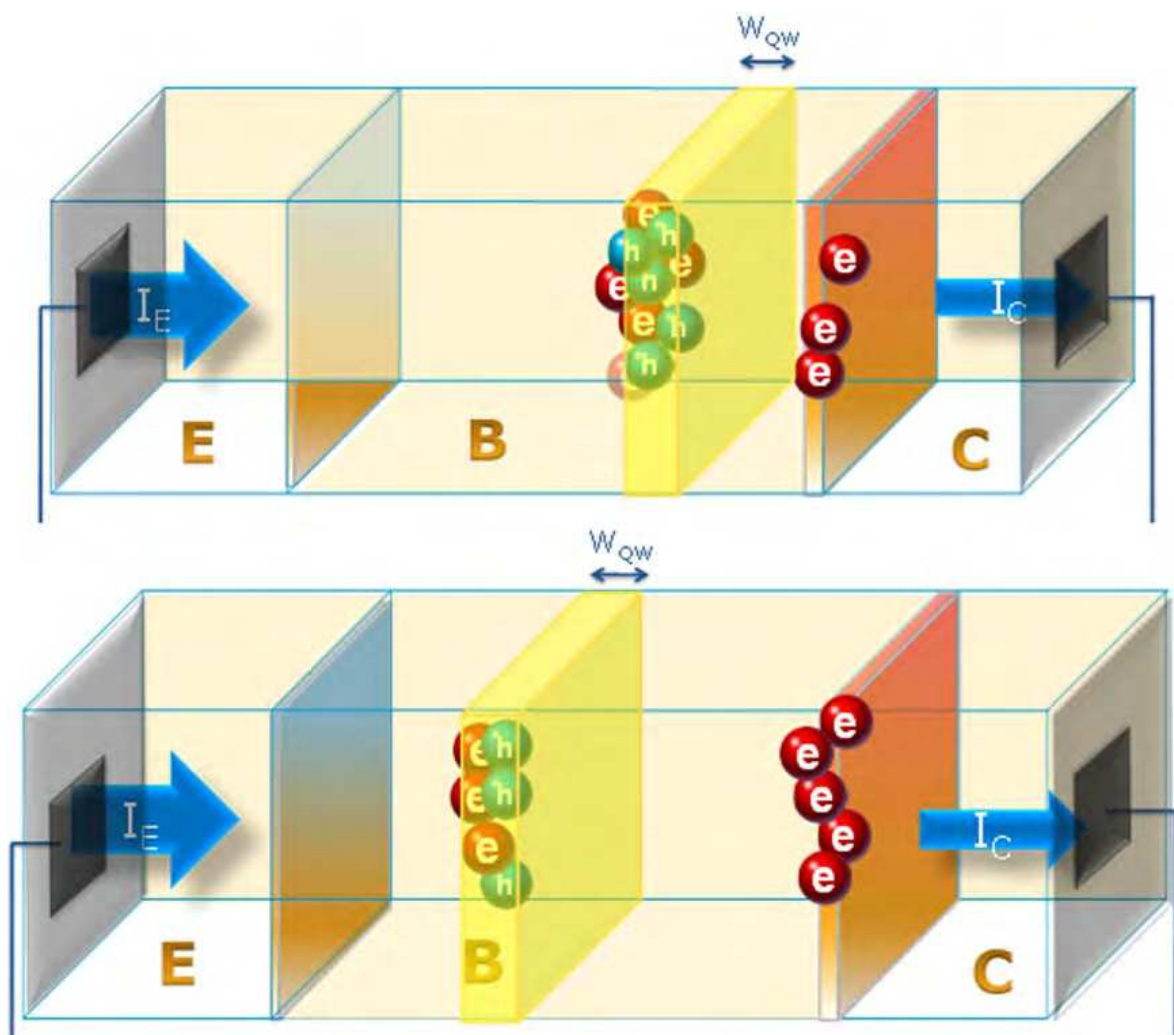


Fig. 7. Animated diagram illustrates a decrease in “trapped” electrons recombined with holes when QW moves from a location near collector (top) towards emitter (down). Carrier “reach time” to QW is thus decreased.

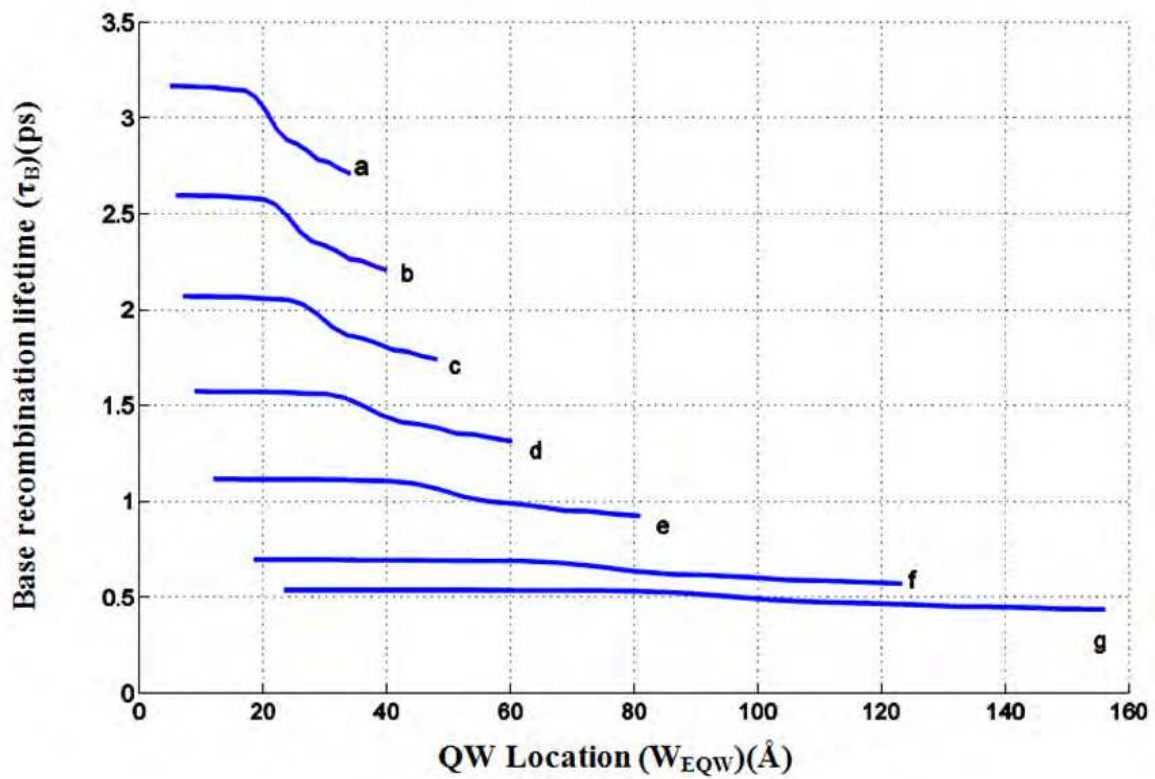


Fig. 8. Calculated base recombination lifetime (τ_B) versus W_{EQW} (a)690 (b)590 (c)490 (d)390 (e)290 (f)190 (g)150(\AA).

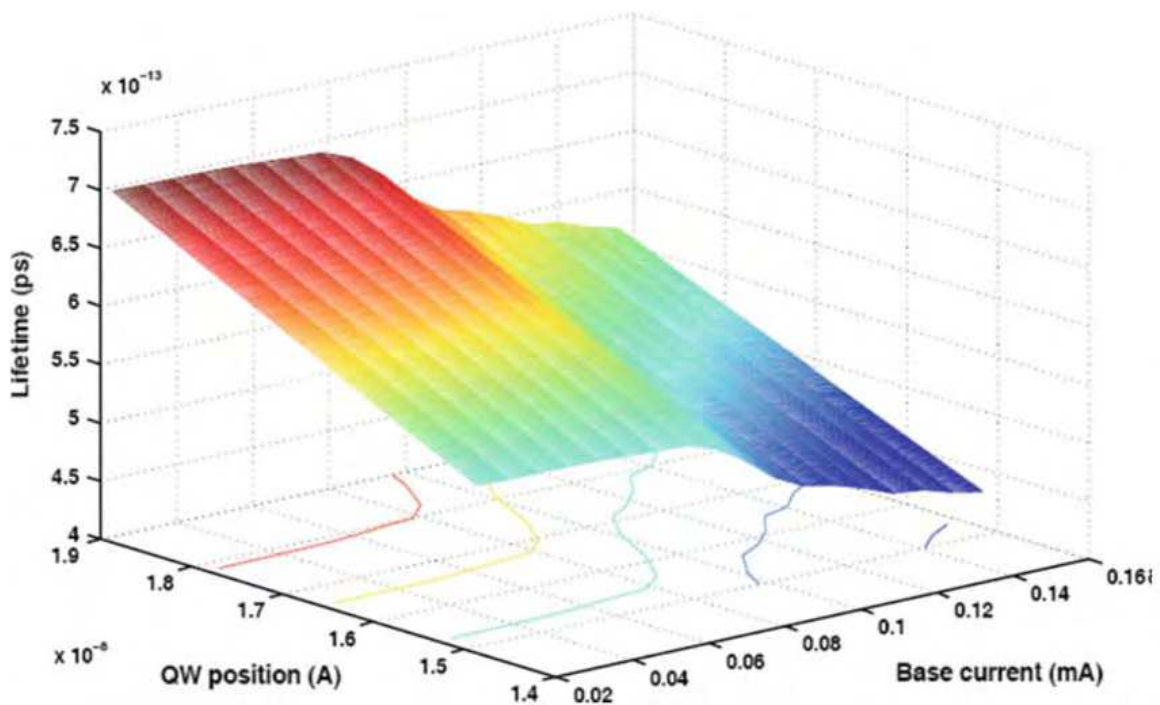


Fig. 9. 3-D scheme of base recombination lifetime (τ_B) versus I_B and W_{EQW} placed in different positions through the base.

5.1.3 Small-signal optical frequency response

Calculating the optical frequency response of transistor laser in 4.1, one can sketch the response for different QW locations. Table 1 shows the simulation results of device parameters for different QW locations through the base region while Fig. 10 and Fig. 11 show optical response and bandwidth dependence on QW location, respectively. As it is obvious from the values for simulated ζ , all of them exceed 0.7 and no resonance peak, the limiting factor for diode lasers, occurs due to QW dislocation through such a thin base layer. Non unity resonance peak in diode lasers with a large carrier lifetime (0.1 - 1 ns), sets limit on f_{-3db} and restricts performance of diode laser.

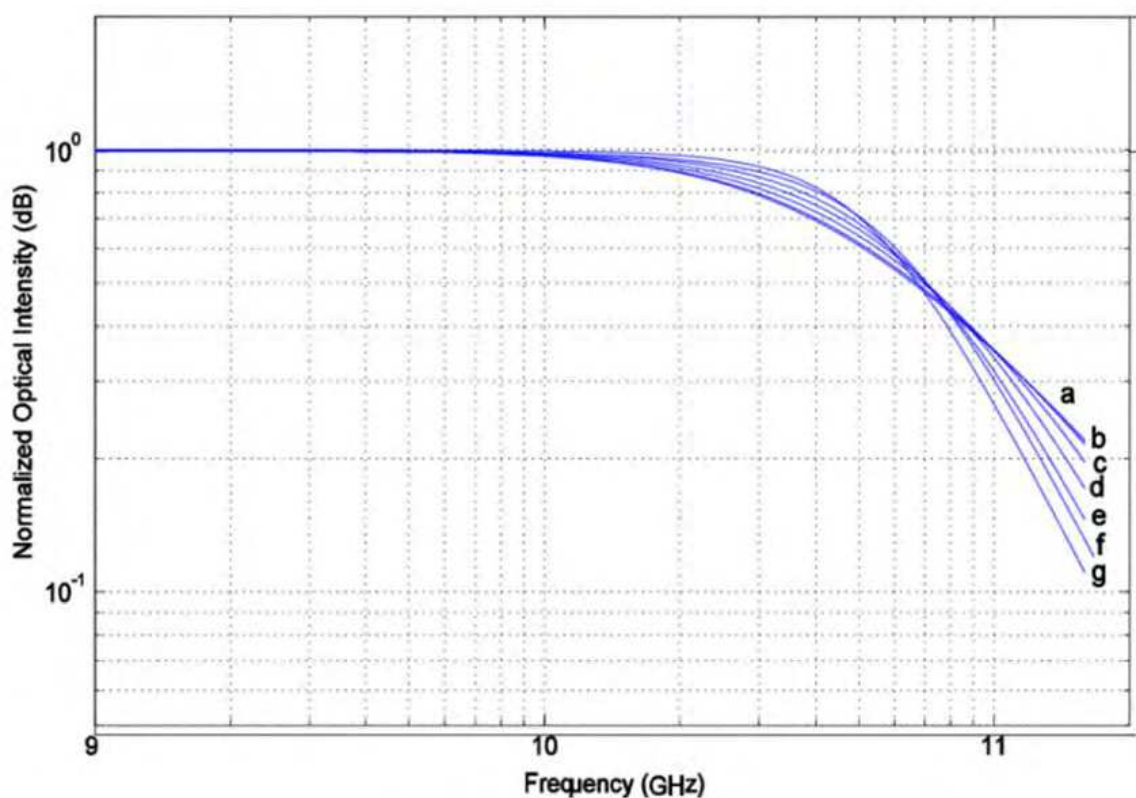


Fig. 10. Optical frequency response for TL with W_{EQW} (a)150 (b)190 (c)290 (d)390 (e)490 (f)590 (g)690(Å).

Increase in optical bandwidth (f_{-3db}) is a direct result of sliding the QW toward collector. At the first glance opposite direction of increase for f_{-3db} and $\tau_{B,spont}$ is confusing and seems mistaken. However, it would be clear if we sketch the f_{-3db} versus $\tau_{B,spont}$ (using approximation of f_{-3db} by equation 18). As Fig. 12 demonstrates, the bandwidth rises abnormally with $\tau_{B,spont}$ increases while reach a peak at about $\tau_{B,spont}=3.37$ ps and then decreases. This fact shines a novel idea that there may be an optimum point for QW to be located in order to maximize the optical bandwidth. Utilizing this figure in conjunction with calculated $\tau_{B,spont}$, one can move the QW toward collector to $W_{EQW}=730$ Å to achieve maximum optical bandwidth (~54 GHz, taking into account the error due to approximate equation). As a result, the QW should be placed closed to collector as much as possible in order to achieve the maximum bandwidth.

Quantum-Well Position (Å)	$\tau_{B,spont}$ (ps)	f_n (undamped natural frequency)(GHz)	ξ (damping ratio)	Simulated -3dB Bandwidth(GHz)
150	0.54	125.8	1.7675	38.7
190	0.7	109.7	1.5595	39.3
290	1.11	87.5	1.2288	42.3
390	1.57	74	1.0365	45.2
490	2.1	64	0.9063	47.4
590	2.57	57	0.8103	48.9
690	3.03	53.5	0.7424	50.9

Table 1. Simulated device parameters for different W_{EQW} ; No resonance peak due to QW movement when $\xi \geq 0.7$.

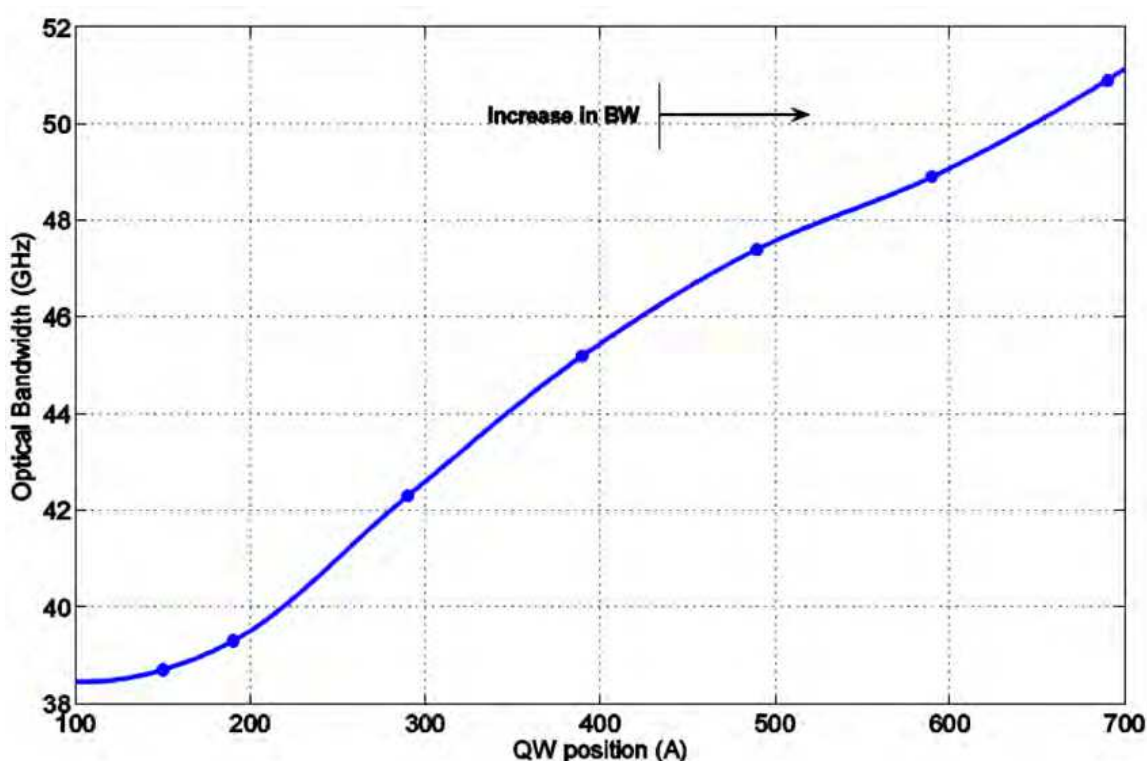


Fig. 11. QW location effect on optical bandwidth; an HBTL with well near its collector has larger optical bandwidth while electrical bandwidth is the same.

5.1.4 Current gain

We predicted previously that optical bandwidth increment would be at cost of sacrificing the current gain (β). Further investigation of QW effect on TL optoelectronic characteristics, this time electrical, leads in an interesting result that matures the previous founding. Collector current gain for an HBTL was calculated in subsection 4.2 in equations (24) and (25). As a result of QW movement towards collector, simulation at constant bias currents shows that τ_{TL} and consequently β declines. Fig. 13 shows this change in optical bandwidth and current gain versus displacement of QW while bias voltage, i.e. v_{be} , forces base current

to be constant at $I_B=33\text{mA}$ for $W_{EQW}=590\text{ \AA}$. This bias enforcement does not disturb generality of the simulation results.

The opposite dependence of BW and β to W_{EQW} , is a trade-off between TL optoelectronic characteristics. Other experimental and theoretical works proved the described “trade-off” between β and f_{-3db} as well (Then et al.,2009),(faraji et al., 2009). They also predict analytically the above mentioned direct dependence of f_{-3db} on $\tau_{B,spont}$. In (Then et al., 2008) the authors utilized an auxiliary base signal to enhance the optical bandwidth. As a merge of their work and the present analysis we can find the optimum place for QW that leads to better results for both β and f_{-3db} of a TL. It means we can use both method, i.e. auxiliary base signal and QW dislocation method, simultaneously. A suggestion for finding an “optimum” QW location consists of two steps . First we focus on β and make it larger by locating the QW close to emitter, e.g. $W_{EQW}<300\text{ \AA}$, which results in $BW<43\text{ GHz}$. Then we use auxiliary AC bias signal to trade some gain for BW. It should be noted that β less than unity is not generally accepted if TL is supposed to work as an electrical amplifier.

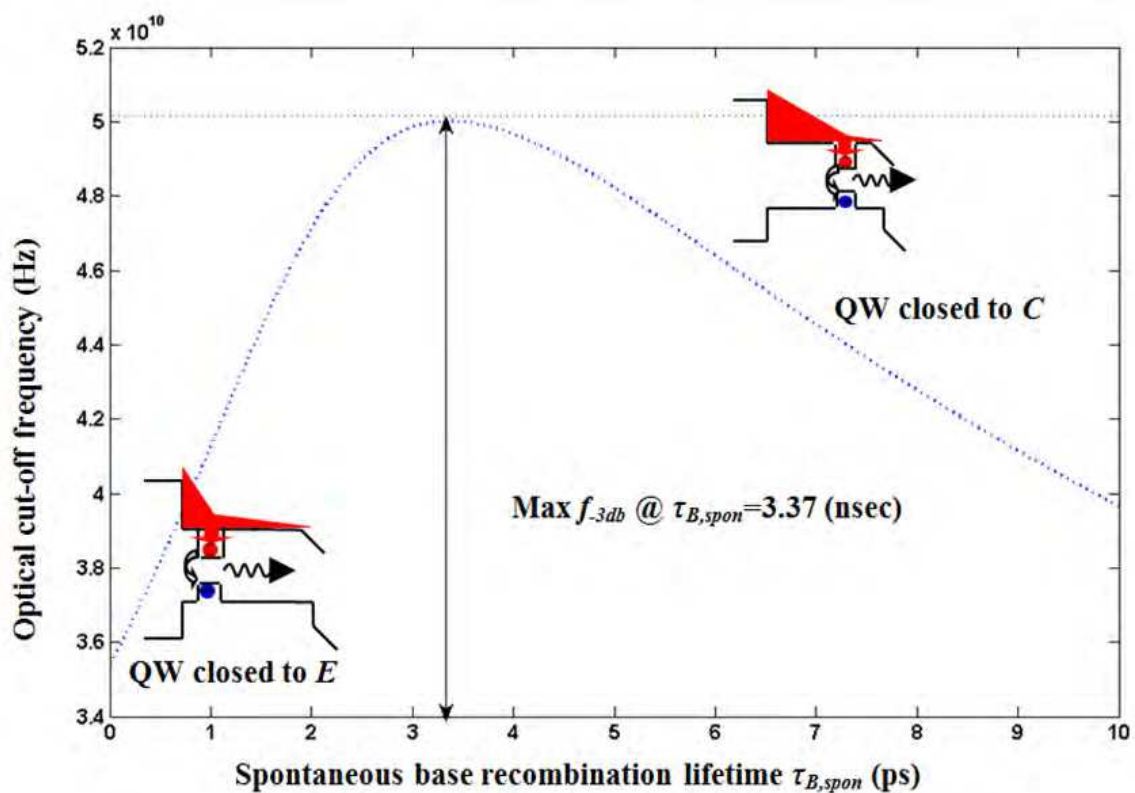


Fig. 12. Calculated optical cut-off frequency (f_{-3db}) versus $\tau_{B,spont}$. Bandwidth is maximum for $\tau_{B,spont}$ corresponding to $W_{EQW}\approx 730\text{ \AA}$.

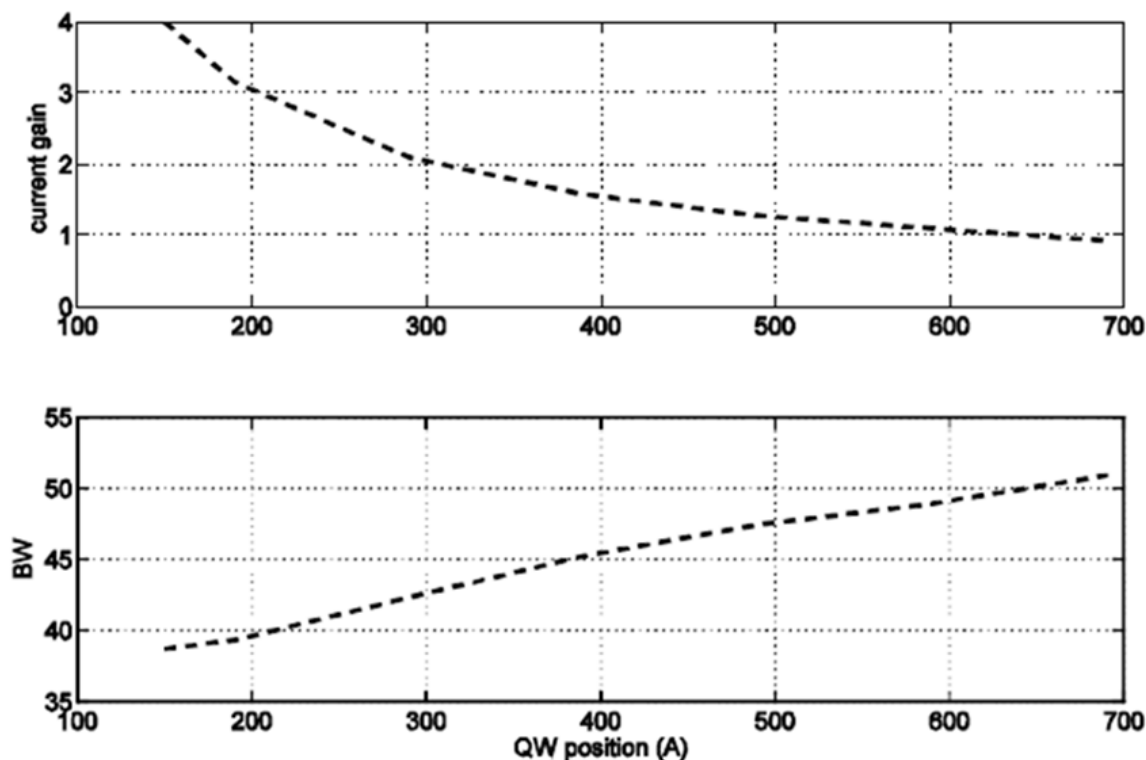


Fig. 13. Electrical gain-optical bandwidth trade-off in an HBT.

5.2 Quantum-well width

Being an optical collector, the QW plays a significant role as it governs both optical and electrical characteristics of TL. Among QW-base geometry parameters, other than QW location, one can investigate the width of QW incorporated within the base region. For instance, we can change the well width while other geometrical parameters, like QW location, are left unchanged in order to examine how the optical frequency response and current gain alter. Base minority carrier recombination lifetime was calculated before as in equation (9) which was an independent function of well width. Charge control model and charge analysis based on this model, described in previous sections, should be completed in order to do this analysis. The base carrier lifetime, τ_B , can be written as below (Then et al., 2007c)

$$1/\tau_B = \sigma v_{th} N_r \tag{28}$$

Where v_{th} is the thermal velocity of carriers, N_r is the density of possible recombination sites and σ is the cross section of carrier capture. σ is a measure of the region that an electron has the possibility to capture and recombine with a hole and is proportional to well width (W_{QW}). In the other hand, N_r depends on the hole concentration, i.e. N_A of the base region. So we can evaluate τ_B as

$$1/\tau_B = GW_{QW}N_A \tag{29}$$

where G is a proportionality factor defined by other geometrical properties of the base. Using this equation one can extract base recombination lifetime of base minority carriers for different base doping densities. Calculations exhibit an indirect relation between τ_B and well

width, agreeing with a larger QW width enhancing the capture cross section for electrons. Moreover, the larger N_A , the greater the recombination and hence the smaller τ_B .

The results for optical frequency response based on Statz-deMars equations of section 4 can be utilized to evaluate the optical properties of a TL for varying well width. Indeed, equations (13) and (14) require $\tau_{B, \text{spont}}$ not τ_B , as described above, therefore threshold current should be calculated for different QW widths. An expression for base threshold current of TL is as below

$$J_{th} = qn_0\tau_{cap}/v\tau_{qw}\tau_{rb} = \frac{qn_0}{\tau_{qw}} \left[1 + \left(\frac{1-v}{v} \right) \frac{\tau_{cap}}{\tau_{rbo}} \right] \quad (30)$$

where n_0 is minority carrier density in steady-state (under dc base current density of J_0), τ_{cap} is the electron capture time by QW (not included in charge control model for simplicity), τ_{qw} is the QW recombination lifetime of electron and τ_{rbo} is the bulk lifetime (or direct recombination lifetime outside the well, also ignored in our model). The base geometry factor, v , gives the fraction of the base charge captured in the QW and defines as (Zhang & Leburton, 2009)

$$v = (W_{qw}/W_b)(1 - x_{qw}/W_b) \quad (31)$$

where W_{qw} is the QW width, the factor we investigate here, W_b is the base width and x_{qw} is the QW location, similar but not equal to previously defined parameter of W_{EQW} . By setting all the constants, one can calculate $\tau_{B, \text{spont}}$ and then small-signal optical frequency response and bandwidth of TL for a range of QW widths. Optimization is also possible like what we did for QW location.

6. Conclusion and future prospects

An analytical simulation was performed to predict dependence of TL optoelectronic characteristics on QW position in order to find a possible optimum place for QW. Simulated base recombination lifetime of HBTL for different QW positions exhibited an increase in optical bandwidth QW moved towards the collector within the base. Further investigations of optical response prove the possibility of a maximum optical bandwidth of about 54GHz in $WEQW \approx 730 \text{ \AA}$. Since no resonance peak occurred in optical frequency response, the bandwidth is not limited in this method. In addition, the current gain decreased when QW moved in the direction of collector. The above mentioned gain-bandwidth trade-off between optoelectronic parameters of TL was utilized together with other experimental methods reported previously to find a QW position for more appropriate performance. The investigated transistor laser has an electrical bandwidth of more than 100GHz. Thus the structure can be modified, utilizing the displacement method reported in this paper, to equalize optical and electrical cut-off frequencies as much as possible.

In previous sections we consider the analysis of a single quantum well (SQW) where there is just one QW incorporated within the base region. This simplifies the modelling and math-related processes. In practice, SQWTL has not sufficient optical gain and may suffer thermal heating which requires additional heat sink. Modifications needed to model a multiple QW transistor laser (MQWTL). First one should rewrite the rate equations of coupled carrier and photon for separate regions between wells. Solving these equations and link them by applying initial conditions, i.e. continuity of current and carrier concentrations, is the next step. In addition to multiple capture and escape lifetime of carriers, tunnelling of the 2-dimensional carriers to the adjacent wells should be considered. For wide barriers one may use carrier transport across the barriers instead the mentioned tunnelling. Simulation results

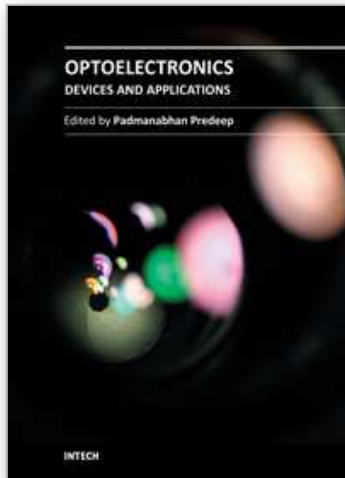
for diode laser (Duan et al., 2010), as one of the transistor laser parents, demonstrate considerable enhancement in optical bandwidth and gain of the device when increasing the number of quantum wells (Nagarajan et al., 1992), (Bahrami and Kaatuzian, 2010). Like the well location modelled here in this chapter, there may be an optimum number of quantum wells to be incorporated within the base region. Due to its high electrical bandwidth (≥ 100 GHz), it is needed to increase the optical modulation bandwidth of the TL. Base region plays the key role in all BJT transistors, especially in Transistor Lasers.

Like Quantum-Well, base structural parameters have significant effects on optoelectronic characteristics of TL which can be modelled like what performed before during this chapter. Among these parameters are base width (Zhang et al., 2009), material, doping (Chu-Kung et al., 2006), etc. For example, a graded base region can cause an internal field which accelerates the carrier transport across the base thus alters both the optical bandwidth and the current gain considerably.

7. References

- Basu, R., Mukhopadhyay, B. & Basu, P.K. (2009). Gain Spectra and Characteristics of a Transistor Laser with InGaAs Quantum Well in the Base. *Proceeding of International Conference on Computers and Devices for Communication*, India, Dec. 2009
- Bahrami Yekta, V. & Kaatuzian, H. (2010). Design considerations to improve high temperature characteristics of $1.3\mu\text{m}$ AlGaInAs-InP uncooled multiple quantum well lasers: Strain in barriers. *Optik, Elsevier*, doi:10.1016/j.ijleo.2010.03.016
- Chan, R., Feng, M., Holonyak, N. Jr., James, A. & Walter, G. (2006). Collector current map of gain and stimulated recombination on the base quantum well transitions of a transistor laser. *Appl. Phys. Lett.*, Vol. 88, No. 143508
- Chu-kung, B.F., Feng, M., Walter, G., Holonyak, N. Jr., Chung, T., Ryou, J.-H., Limb, J., Yoo, D., Shen, S.C. & Dupuis, R.D. (2006). Graded-base InGaN/GaN heterojunction bipolar light-emitting transistors. *Appl. Phys. Lett.* Vol. 89, No. 082108
- Dixon, F., Feng, M. & Holonyak, N. Jr. (2010). Distributed feedback transistor laser. *Appl. Phys. Lett.* Vol. 96, No. 241103
- Dixon, F., Chan, R., Walter, G., Holonyak, N. Jr. & Feng, M. (2006). Visible spectrum light-emitting transistors. *Appl. Phys. Lett.* Vol. 88, No. 012108
- Duan, Z., Shi, W., Chrostowski, L., Huang, X., Zhou, N., & Chai, G. (2010). Design and epitaxy of $1.5\mu\text{m}$ InGaAsP-InP MQW material for a transistor laser. *Optics Express*, Vol. 18, Issue 2, pp. (1501-1509), doi:10.1364/OE.18.001501
- Faraji, B., Pulfrey, D.L. & Chrostowski, L. (2008). Small-signal modeling of the transistor laser including the quantum capture and escape lifetimes. *Appl. Phys. Lett.*, Vol. 93, No. 103509
- Faraji, B., Shi, W., Pulfrey, D.L. & Chrostowski, L. (2009). Analytical modeling of the transistor laser. *IEEE Journal of Quantum Electron.*, Vol. 15, No. 3, pp (594-603)
- Feng, M., Holonyak, N. Jr. & Hafez, W. (2004a). Light-emitting transistor: light emission from InGaP/GaAs heterojunction bipolar transistors. *Appl. Phys. Lett.* Vol. 84, No. 151
- Feng, M., Holonyak, N. Jr. & Chan, R. (2004b). Quantum-well-base heterojunction bipolar light-emitting transistor. *Appl. Phys. Lett.*, Vol. 84, No. 11
- Feng, M., Holonyak, N. Jr., Walter, G. & Chan, R. (2005). Room temperature continuous wave operation of a heterojunction bipolar transistor laser. *Appl. Phys. Lett.* Vol. 87, No. 131103

- Feng, M., Holonyak, N. Jr., Chan, R., James, A. & Walter, G. (2006a). Signal mixing in a multiple input transistor laser near threshold. *Appl. Phys. Lett.* Vol. 88, No. 063509
- Feng, M., Holonyak, N. Jr., James, A., Cimino, K., Walter, G. & Chan, R. (2006b). Carrier lifetime and modulation bandwidth of a quantum well AlGaAs/InGaP/GaAs/InGaAs transistor laser. *Appl. Phys. Lett.* Vol. 89, No. 113504
- Feng, M., Holonyak, N. Jr., Then, H.W. & Walter, G. (2007). Charge control analysis of transistor laser operation. *Appl. Phys. Lett.* Vol. 91, No. 053501
- Feng, M., Holonyak, N. Jr., Then, H.W., Wu, C.H. & Walter, G. (2009). Tunnel junction transistor laser. *Appl. Phys. Lett.* Vol. 94, No. 041118
- Kaatuzian, H. (2005). *Photonics, Vol. 1*, AmirKabir University of Technology press, , Tehran, Iran
- Kaatuzian, H. & Taghavi,I. (2009). Simulation of quantum-well slipping effect on optical bandwidth in transistor laser. *Chinese optics letters*. doi:10.3788/COL20090705.0435, pp. 435–436
- Nagarajan, R., Ishikawa, M., Fukushima, T., Geels, R. & Bowers, E. (1992). High speed quantum-well lasers and carrier transport effects. *IEEE Journal of Quantum Electron*, Vol. 28, No. 10, pp (1990-2008)
- Shi, W., Chrostowski, L & Faraji, B. (2008). Numerical Study of the Optical Saturation and Voltage Control of a Transistor Vertical-Cavity Surface-Emitting Laser. *IEEE Photonics Technology Letters*, Vol. 20, No. 24
- Suzuki, Y., Yajima, H., Shimoyama, K., Inoue, Y., Katoh, M. & Gotoh, H. (1990). (Heterojunction field effect transistor laser). *Ellectronics Letters*, Vol. 26, No. 19
- Taghavi,I & Kaatuzian, H. (2010). Gain-Bandwidth trade-off in a transistor laser : quantum well dislocation effect. *Springer, Opt Quant Electron*. doi: 10.1007/s11082-010-9384-0, pp. 481–488
- Then, H.W., Walter, G., Feng, M. & Holonyak, N. Jr. (2007a). Collector characteristics and the differential optical gain of a quantum-well transistor laser. *Appl. Phys. Lett* Vol. 91, No. 243508
- Then, H.W., Feng, M. & Holonyak, N. Jr. (2007b). Optical bandwidth enhancement by operation and modulation of the first excited state of a transistor laser. *Appl. Phys. Lett.* Vol. 91, No. 183505
- Then, H.W., Feng, M., Holonyak, N. Jr. & Wu, C.H. (2007c). Experimental determination of the effective minority carrier lifetime in the operation of a quantum-well n-p-n heterojunction bipolar light-emitting transistor of varying base quantum-well design and doping. *Appl. Phys. Lett.* Vol. 91, No. 033505
- Then, H.W., Walter, G., Feng, M. & Holonyak, N. Jr. (2008). Optical bandwidth enhancement of heterojunction bipolar transistor laser operation with an auxiliary base signal. *Appl. Phys. Lett.* Vol. 93, No. 163504
- Then, H.W., Feng, M. & Holonyak, N. Jr. (2009). Bandwidth extension by trade-off of electrical and optical gain in a transistor laser: three-terminal control. *Appl. Phys. Lett.* Vol. 94, No. 013509
- Then, H.W., Feng, M. & Holonyak, N. Jr. (2010). Microwave circuit model of the three-port transistor laser. *Appl. Phys. Lett.* Vol. 107, No. 094509
- Walter, G., Holonyak, N. Jr., Feng, M. & Chan, M. (2004). Laser operation of a heterojunction bipolar light-emitting transistor. *Appl. Phys. Lett.* Vol. 85, No. 4768
- Walter, G., James, A., Holonyak, N. Jr., Feng, M. & Chan, R. (2006). Collector breakdown in the heterojunction bipolar transistor laser. *Appl. Phys. Lett.* Vol. 88, No. 232105
- Zhang, L. & Leburton, J.-P. (2009). Modeling of the transient characteristics of heterojunction bipolar transistor lasers. *IEEE Journal of Quantum Electron*. doi:10.1109/JQE.2009.2013215, pp. (359–366)



Optoelectronics - Devices and Applications

Edited by Prof. P. Predeep

ISBN 978-953-307-576-1

Hard cover, 630 pages

Publisher InTech

Published online 03, October, 2011

Published in print edition October, 2011

Optoelectronics - Devices and Applications is the second part of an edited anthology on the multifaced areas of optoelectronics by a selected group of authors including promising novices to experts in the field. Photonics and optoelectronics are making an impact multiple times as the semiconductor revolution made on the quality of our life. In telecommunication, entertainment devices, computational techniques, clean energy harvesting, medical instrumentation, materials and device characterization and scores of other areas of R&D the science of optics and electronics get coupled by fine technology advances to make incredibly large strides. The technology of light has advanced to a stage where disciplines sans boundaries are finding it indispensable. New design concepts are fast emerging and being tested and applications developed in an unimaginable pace and speed. The wide spectrum of topics related to optoelectronics and photonics presented here is sure to make this collection of essays extremely useful to students and other stake holders in the field such as researchers and device designers.

How to reference

In order to correctly reference this scholarly work, feel free to copy and paste the following:

Iman Taghavi and Hassan Kaatuzian (2011). Effects of Quantum-Well Base Geometry on Optoelectronic Characteristics of Transistor Laser, Optoelectronics - Devices and Applications, Prof. P. Predeep (Ed.), ISBN: 978-953-307-576-1, InTech, Available from: <http://www.intechopen.com/books/optoelectronics-devices-and-applications/effects-of-quantum-well-base-geometry-on-optoelectronic-characteristics-of-transistor-laser>

INTECH
open science | open minds

InTech Europe

University Campus STeP Ri
Slavka Krautzeka 83/A
51000 Rijeka, Croatia
Phone: +385 (51) 770 447
Fax: +385 (51) 686 166
www.intechopen.com

InTech China

Unit 405, Office Block, Hotel Equatorial Shanghai
No.65, Yan An Road (West), Shanghai, 200040, China
中国上海市延安西路65号上海国际贵都大饭店办公楼405单元
Phone: +86-21-62489820
Fax: +86-21-62489821

© 2011 The Author(s). Licensee IntechOpen. This is an open access article distributed under the terms of the [Creative Commons Attribution 3.0 License](#), which permits unrestricted use, distribution, and reproduction in any medium, provided the original work is properly cited.

IntechOpen

IntechOpen